Journal of Photochemistry and Photobiology A: Chemistry 340 (2017) 80–87

Contents lists available at ScienceDirect

Journal of Photochemistry and Photobiology A: Chemistry

journal homepage: www.elsevier.com/locate/jphotochem

Invited feature article

Self-assembly through hydrogen bonding and photochemical properties of supramolecular complexes of bis(18-crown-6)stilbene with alkanediammonium ions

Evgeny N. Ushakov[a,b,*], Timofey P. Martyanov[a,b], Artem I. Vedernikov[b], Oleg V. Pikalov[a,b], Asya A. Efremova[b], Lyudmila G. Kuz'mina[c], Judith A.K. Howard[d], Michael V. Alfimov[b], Sergey P. Gromov[b,*]

[a] Institute of Problems of Chemical Physics, Russian Academy of Sciences, Chernogolovka 142432, Moscow Region, Russian Federation
[b] Photochemistry Center, Russian Academy of Sciences, Novatorov str. 7A-1, Moscow 119421, Russian Federation
[c] N. S. Kurnakov Institute of General and Inorganic Chemistry, Russian Academy of Sciences, Leninskiy prosp. 31, Moscow 119991, Russian Federation
[d] Department of Chemistry, Durham University, South Road, Durham DH1 3LE, United Kingdom

ARTICLE INFO

Article history:
Received 26 October 2016
Received in revised form 7 February 2017
Accepted 2 March 2017
Available online 7 March 2017

Keywords:
Bis(18-crown-6)stilbene
Alkanediammonium ions
Hydrogen-bonded complexes
Bis-pseudosandwich complexes
Supramolecular [2+2] photocycloaddition
E–Z photoisomerization

ABSTRACT

Binding of alkanediammonium ions $^{+}H_3N(CH_2)_nNH_3^{+}$, $n = 2–6$, to (*E*)-bis(18-crown-6)stilbene initiates the [2+2] photocycloaddition reaction leading mainly to the *rctt* isomer of 1,2,3,4-tetrakis(benzo-18-crown-6)cyclobutane. The high efficiency and stereoselectivity of this photoreaction in dilute solution are due to the formation of bis-pseudosandwich complexes consisting of two stilbene molecules and two alkanediammonium ions. With a decrease in the length of the polymethylene spacers in the 2:2 complex, the quantum yield of supramolecular [2+2] photocycloaddition increases from 0.02 to 0.27, while the quantum yield of the competing *E–Z* photoisomerization decreases from 0.12 to 0.06. Spectrophotometric observations and density functional theory calculations revealed that (*Z*)-bis(18-crown-6)stilbene, unlike the *E* isomer, is able to form pseudocyclic 1:1 complexes with $^{+}H_3N(CH_2)_nNH_3^{+}$, $n = 2–6$, owing to the proximity of two crown ether moieties. The peculiar spectral properties of these complexes are associated with large torsion angles around the ethylene–benzocrown single bonds. X-ray diffraction analysis showed that co-crystallization of (*E*)-bis(18-crown-6)stilbene with 1,6-hexanediammonium diperchlorate affords a linear polymer in which the alternating stilbene molecules and diammonium ions are connected by hydrogen bonds.

1. Introduction

The [2+2] photocycloaddition (PCA) reaction of olefins is one of the few photoreactions widely used in organic synthesis [1], in particular, in the synthesis of pharmaceutical and natural products [2]. The intermolecular PCA reactions in solution are normally characterized by very low quantum yields, because of short excited state lifetime, and afford a mixture of cyclobutane isomers. This is especially true for acyclic olefins able to undergo the *E–Z* photoisomerization reaction. The self-assembly of reactants into supramolecular arrays *via* noncovalent interactions is an efficient tool for controlling PCA [3]. Recent reviews [4,5] cover the key methods that are used to obtain assemblies of unsaturated compounds pre-organized for this photoreaction in solution: cation-induced self-assembly, confinement of reactants in supramolecular containers, self-assembly through hydrogen bonding, and so on. One of the most studied methods is cation-induced self-assembly of unsaturated compounds modified by ligand groups to form dimeric, pseudodimeric, and sandwich complexes [5]. It can provide both high efficiency and stereoselectivity of the PCA reaction even in the case of acyclic compounds, such as 1,3-butadienes [6], owing to relatively strong non-covalent contacts of reactants.

Previously, it was shown [7] that the *E* isomer of bis(18-crown-6)stilbene ((*E*)-**1**) is able to form pseudocyclic complexes of 2:2 composition (bis-pseudosandwich complexes) with alkanediammonium ions of the structure $^{+}H_3N(CH_2)_nNH_3^{+}$ ($\mathbf{C}_n^{2+}$), where $n = 2–6$. The photoirradiation of complexes [(*E*)-**1**·$\mathbf{C}_n^{2+}$]$_2$, $n = 2–6$, in

* Corresponding authors at: Photochemistry Center, Russian Academy of Sciences, Novatorov str. 7A-1, Moscow 119421, Russian Federation.
E-mail addresses: e.n.ushakov@gmail.com (E.N. Ushakov), spgromov@mail.ru (S.P. Gromov).

http://dx.doi.org/10.1016/j.jphotochem.2017.03.003
1010-6030/

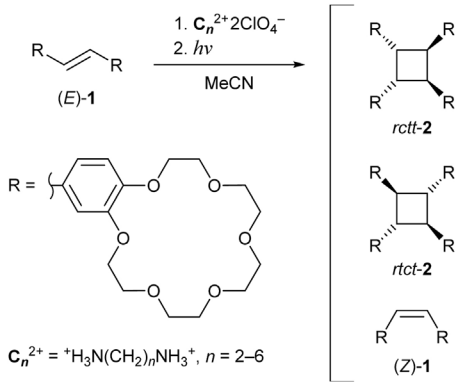

Scheme 1. Supramolecular synthesis of tetrakis(benzo-18-crown-6)cyclobutane.

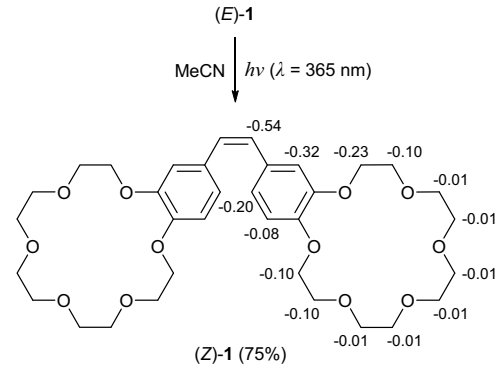

Scheme 2. Synthesis of (*Z*)-**1** and differences in the proton chemical shifts of (*Z*)-**1** and (*E*)-**1**; $\Delta\delta_H$ (ppm) = $\delta_H(Z) - \delta_H(E)$, 2×10^{-3} M, MeCN-d_3, 25 °C.

MeCN afforded the *Z* isomer of bis(18-crown-6)stilbene ((*Z*)-**1**) and two cyclobutane isomers *rctt*-**2** and *rtct*-**2** (Scheme 1); the relative yield of the *rctt* isomer reached 95% (in the case of $\mathbf{C_3}^{2+}$).

Among variety of reports on supramolecular PCA reactions, only a few contain quantitative information about structure–property relationships [8]. The key goals of this study were to elucidate a detailed picture of the hydrogen bond-directed self-assembly of bis(18-crown-6)stilbene and alkanediammonium ions into supramolecular complexes of various composition and structure, and to determine how the length of the polymethylene spacers in the bis-pseudosandwich complexes [(*E*)-**1**·$\mathbf{C_n}^{2+}$]$_2$ affects the quantum yields of the competing PCA and *E*–*Z* photoisomerization reactions of (*E*)-**1**.

2. Experimental

2.1. General methods

^{1}H and ^{13}C NMR spectra were recorded on a Bruker DRX500 spectrometer (500 and 125 MHz, respectively) in DMSO-d_6 and MeCN-d_3 at 25–30 °C using the solvent as the internal standard (δ_H 2.50 and δ_C 39.43 for DMSO-d_6 and δ_H 1.96 for MeCN-d_3). 2D COSY and NOESY spectra and ^{1}H–^{13}C heteronuclear correlation (HSQC and HMBC) spectra were used to assign the proton and carbon signals. Melting points (uncorrected) were measured in capillaries on a Mel-Temp II instrument. The samples for elemental analyses were dried *in vacuo* at 80 °C. Electronic absorption spectra were measured on a Specord-M40 spectrophotometer in 0.1, 1, and 5 cm quartz cells with ground-in stoppers. All manipulations with solutions containing bis(18-crown-6)stilbene were performed in a darkroom under red light (daylight induces the *E*–*Z* photoisomerization of bis(18-crown-6)stilbene in solution). Stationary photolysis was performed using glass-filtered light of a high pressure Hg lamp (λ = 365 nm). The light intensity was measured by chemical actinometry.

2.2. Synthesis

Compounds $\mathbf{C_n}^{2+}2ClO_4^-$, *n* = 2–6, were obtained according to known procedures [7,9]. Stilbene (*E*)-**1** was prepared by the facile and high-performance method developed previously [10]. Solid complexes (*E*)-**1**·$\mathbf{C_n}^{2+}2ClO_4^-$, *n* = 2, 5, 6, were obtained by slow crystallization of equimolar mixtures of the components; according to elemental analysis data, all these complexes have formally 1:1 stoichiometry (Supplementary data). The *Z* isomer of stilbene **1** was prepared by irradiation of an acetonitrile solution of (*E*)-**1** with 365 nm light (Scheme 2) followed by removal of the remaining *E* isomer by precipitation with hexane from a benzene solution. It is noteworthy that (*Z*)-**1** was obtained as a solid; this attests to a higher purity of this sample compared with the previously described (*Z*)-**1** sample [11], which was isolated as an oil. The ^{1}H NMR signals of aromatic and ethylene protons of (*Z*)-**1** are shifted upfield relative to the corresponding signals of (*E*)-**1** (Scheme 2). The main reason is that the stilbene moiety in (*Z*)-**1** is non-planar as a result of steric interaction between the aryl residues and, hence, the conjugation in this moiety is disrupted.

18,18′-[(*Z*)-Ethene-1,2-diyl]bis(2,3,5,6,8,9,11,12,14,15-decahydro-1,4,7,10,13,16-benzohexaoxacyclooctadecine) (stilbene (*Z*)-**1**). Stilbene (*E*)-**1** (20 mg, 30.9 μmol) was dissolved in 60 mL of MeCN. Four portions of this solution (15 mL each) were irradiated with 365 nm light in a non-standard quartz cell (15 cm height, 10 cm width, and 0.1 cm optical path length) until the photostationary equilibrium between *E* and *Z* isomers was attained (spectrophotometric monitoring). The photostationary mixtures were combined, the solvent was evaporated *in vacuo*, and the residue was dissolved in benzene (5 mL). After addition of hexane (5 mL), the precipitated (*E*)-**1** was filtered off. The mother liquor was concentrated *in vacuo* and the residue was again dissolved in benzene (2.5 mL). After addition of hexane (5 mL) and cooling to 5 °C, the precipitated (*E*)-**1** was filtered off. The mother liquor was then evaporated *in vacuo* to give (*Z*)-**1** (15 mg, yield 75%) as a colorless glassy substance, which slowly solidified when kept in the dark, mp 79–82 °C (*cf.* lit. [11]: colorless oil). Calcd for $C_{34}H_{48}O_{12}$: C, 62.95; H, 7.46%. Found: C, 63.14; H, 7.31%. MS, *m*/*z* (I_{rel} (%)): 648 [M]$^+$ (100), 148 (5), 111 (5), 98 (10), 83 (22), 73 (12), 57 (24), 56 (15), 55 (29).

^{1}H NMR (DMSO-d_6) δ (ppm) 3.52 (s, 8 H, 4 CH_2O), 3.54 (m, 8 H, 4 CH_2O), 3.58 (m, 8 H, 4 CH_2O), 3.66 (m, 4 H, 2 14-C*H*$_2$CH$_2$OAr), 3.72 (m, 4 H, 2 3-C*H*$_2$CH$_2$OAr), 3.88 (m, 4 H, 2 15-C*H*$_2$OAr), 4.04 (m, 4 H, 2 2-C*H*$_2$OAr), 6.44 (s, 2 H, (*Z*)-HC=CH), 6.78 (dd, ^3J = 8.2 Hz, ^4J = 1.8 Hz, 2 H, 2 19-H), 6.82 (d, ^4J = 1.8 Hz, 2 H, 2 17-H), 6.87 (d, ^3J = 8.2 Hz, 2 H, 2 20-H).

^{13}C NMR (DMSO-d_6) δ (ppm) 67.81 (2 15-*C*H$_2$OAr), 68.00 (2 2-*C*H$_2$OAr), 68.53 (2 14-*C*H$_2$CH$_2$OAr), 68.64 (2 3-*C*H$_2$CH$_2$OAr), 69.73 (12 CH_2O), 112.81 (2 20-C), 113.31 (2 17-C), 121.35 (2 19-C), 128.41 ((*Z*)-HC=CH), 129.63 (2 18-C), 147.36 (2 20a-C), 147.57 (2 16a-C).

2.3. Computational details

The molecular structures of (*Z*)-**1** and complexes (*Z*)-**1**·(EtNH$_3^+$)$_2$ and (*Z*)-**1**·$\mathbf{C_2}^{2+}$ in MeCN were calculated as follows. At first, four C_2-symmetrical conformers of (*Z*)-**1** were constructed using benzo-18-crown-6 ether molecule in its typical conformation. These are (*s-trans*)$_2$-(*up*)$_2$, (*s-trans*)$_2$-(*dn*)$_2$, (*s-cis*)$_2$-(*up*)$_2$, and (*s-cis*)$_2$-(*dn*)$_2$ (see Fig. 1). The geometries of these conformers were optimized in the gas phase using the parameterized electronic structure model developed by Laikov [12] and implemented in the Priroda 14 program [13]. The optimized structures were used to

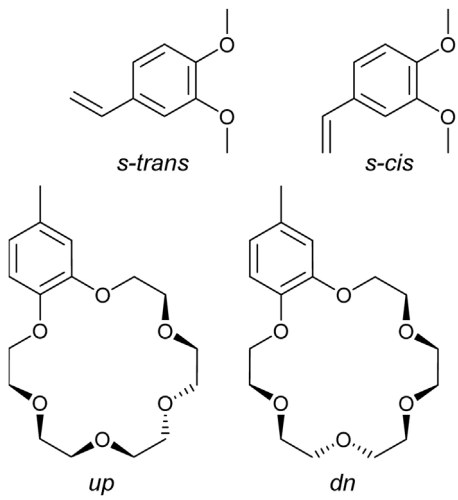

Fig. 1. Conformational notation.

generate other symmetrical and asymmetrical conformers of (*Z*)-**1** by 180° rotation of the benzocrown ether moieties around the single bonds connecting these moieties to the olefinic bond. To construct the ammonium and diammonium complexes we used only symmetrical conformers of (*Z*)-**1**. All the initial structures were optimized by the method developed by Laikov.

The subsequent density functional theory (DFT) calculations were performed using the Gaussian 09 program package [14]. DFT geometry optimizations were first carried out using loose convergence criteria to select a few most probable conformations for each of the three compounds. In these calculations we used the M06-2X functional [15], the 6-31G(d) basis set, and the SMD polarizable continuum model [16] in order to simulate effects of MeCN as the experimental solvent. These preliminary studies revealed that more compact (*s-cis*)$_2$ conformations of stilbene (*Z*)-**1** (in both free and bound states) should predominate in the polar solvent. For the selected conformations, the free energies in solution were calculated to determine the most stable conformer.

In continuum solvation models the free energy in solution is expressed as follows [17]:

$$G_{soln} = E_{soln} + G_{nes} + \Delta G_{corr\_gas}$$

where E_{soln} is the electronic energy of the solute in the presence of the solvent field, G_{nes} is the sum of nonelectrostatic contributions to the solvation free energy, and ΔG_{corr_gas} is the thermal correction to the free energy of the solute in the gas phase.

To calculate G_{soln}, molecular geometries were fully optimized both in solution and in the gas phase using the M06-2X/6-31G(d) method. The optimizations in the gas-phase were followed by analytical frequency calculations at the same level of theory to estimate ΔG_{corr_gas} at 298 K. The thermochemical analysis was carried out using a scale factor of 0.97 for harmonic frequencies. The sum of E_{soln} and G_{nes} was derived from single-point energy calculation with the relatively large 6-311++G(d,p) basis set in order to reduce basis set incompleteness errors.

The free energies of the $EtNH_3^+$ and $\mathbf{C_2}^{2+}$ ions in solution were also calculated by the same method in order to estimate the binding free energies for complexes (*Z*)-**1**·$(EtNH_3^+)_2$ and (*Z*)-**1**·$\mathbf{C_2}^{2+}$:

$$\Delta G_{bind}|L\cdot(A^{n+})_m| = G_{soln}|L\cdot(A^{n+})_m| - G_{soln}|L| - mG_{soln}|A^{n+}|$$

where L is the (*Z*)-**1** molecule, A^{n+} is the cation, n, $m = 1, 2$. The calculated G_{soln} and ΔG_{bind} values are given in Table S1 (Supplementary data).

The calculations of the S_0–S_1 electronic transition energies in solution were performed on the ground-state geometries optimized at the M06-2X/6-31G(d)/SMD level of theory using the time-dependent DFT (TDDFT) method [18] with the same functional, basis set, and solvation model.

3. Results and discussion

3.1. Absorption spectral properties

The formation of bis-pseudosandwich complexes of (*E*)-**1** with $\mathbf{C_n}^{2+}$ in dilute solution can be represented as two successive equilibrium reactions:

$$(E) - \mathbf{1} + \mathbf{C_n}^{2+} \overset{K_{1:1}}{\rightleftharpoons} (E) - \mathbf{1}\cdot\mathbf{C_n}^{2+} \quad (1)$$

$$(E) - \mathbf{1}\cdot\mathbf{C_n}^{2+} + (E) - \mathbf{1}\cdot\mathbf{C_n}^{2+} \overset{K_{2:2}}{\rightleftharpoons} [(E) - \mathbf{1}\cdot\mathbf{C_n}^{2+}]_2 \quad (2)$$

The second reaction occurs between two dications; therefore, as the solution ionic strength increases, equilibrium (2) should shift toward the 2:2 complex. In order to achieve the highest relative content of this complex, we conducted the spectroscopic and photochemical measurements for systems (*E*)-**1**–$\mathbf{C_n}^{2+}$ at a constant high ionic strength (0.01 M, supporting electrolyte $Bu_4N^+ClO_4^-$) and rather high total concentrations of (*E*)-**1** (about 3.5×10^{-4} M) and $\mathbf{C_n}^{2+}$ (about 5.5×10^{-4} M).

The $K_{1:1}$ and $K_{2:2}$ constants for the (*E*)-**1**–$\mathbf{C_n}^{2+}$ systems in MeCN could not be determined by direct spectrophotometric titration because of too high $K_{2:2}$ values and small differences between the spectra of [(*E*)-**1**·$\mathbf{C_n}^{2+}$]$_2$ and (*E*)-**1**·$\mathbf{C_n}^{2+}$. Published data [7–9,19] suggest that in these systems, $K_{1:1} > 10^4\ M^{-1}$ and $K_{2:2} > 10^7\ M^{-1}$. Then at the above-indicated reactant concentrations, at least 98% of (*E*)-**1** should exist as the complex [(*E*)-**1**·$\mathbf{C_n}^{2+}$]$_2$. This suggestion is supported by photochemical data (see Section 3.2).

Fig. 2 (solid curves) shows the absorption spectra of stilbene (*E*)-**1** and complexes [(*E*)-**1**·$\mathbf{C_2}^{2+}$]$_2$ and (*E*)-**1**·$(EtNH_3^+)_2$ in MeCN. Complete conversion of (*E*)-**1** to (*E*)-**1**·$(EtNH_3^+)_2$ was reached when a large excess of $EtNH_3^+ClO_4^-$ (0.01 M) over (*E*)-**1** was used (spectrophotometric titration data). The formation of complexes [(*E*)-**1**·$\mathbf{C_2}^{2+}$]$_2$ and (*E*)-**1**·$(EtNH_3^+)_2$ leads only to a minor hypsochromic shift of the long-wavelength absorption band of (*E*)-**1**. The bis-pseudosandwich complex [(*E*)-**1**·$\mathbf{C_2}^{2+}$]$_2$ demonstrates a less intense but broader absorption band in comparison with (*E*)-**1**·$(EtNH_3^+)_2$. This fact is attributable to the stacking interactions between the two stilbene moieties of [(*E*)-**1**·$\mathbf{C_2}^{2+}$]$_2$. As the number of methylene units in $\mathbf{C_n}^{2+}$ increases, the absorption band of the 2:2

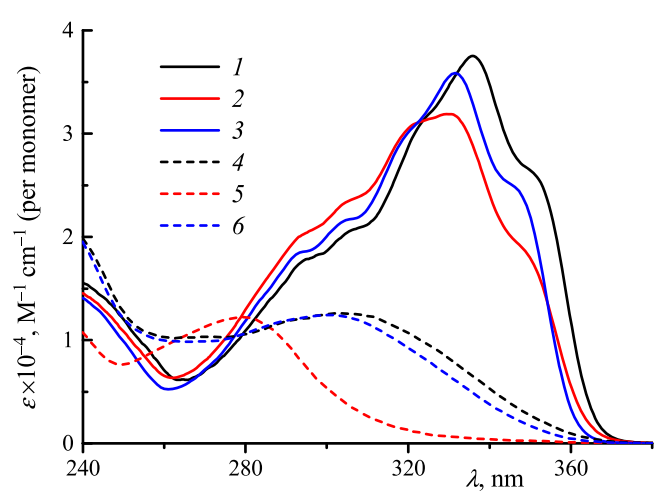

Fig. 2. Absorption spectra of (*E*)-**1** (*1*), [(*E*)-**1**·$\mathbf{C_2}^{2+}$]$_2$ (*2*), (*E*)-**1**·$(EtNH_3^+)_2$ (*3*), (*Z*)-**1** (*4*), (*Z*)-**1**·$\mathbf{C_2}^{2+}$ (*5*), and (*Z*)-**1**·$(EtNH_3^+)_2$ (*6*) in MeCN.

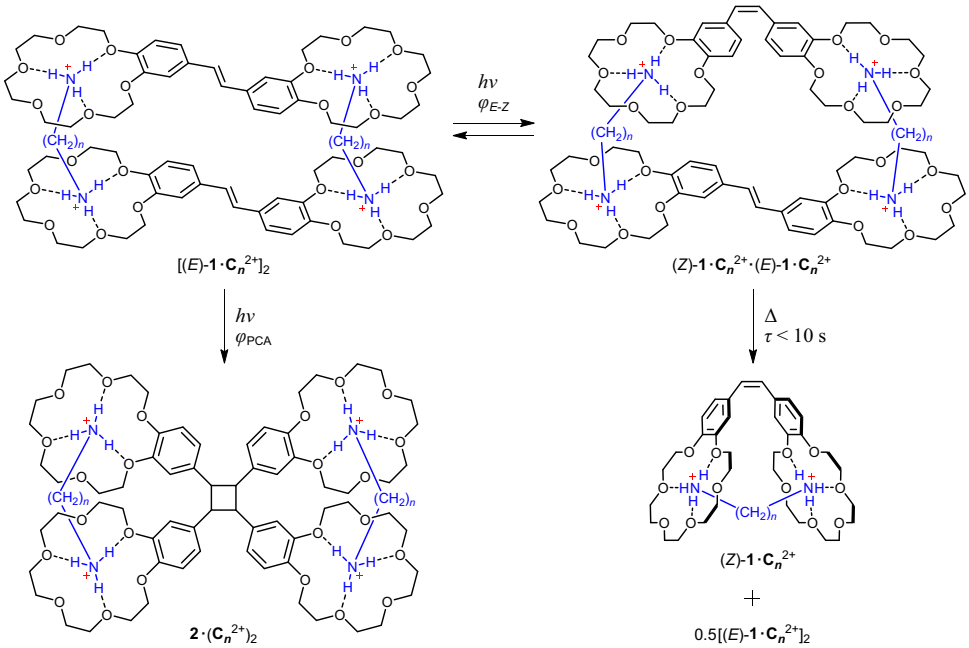

Scheme 3. Photochemical and thermal processes occurring during stationary irradiation of complexes [(*E*)-**1**·$\mathbf{C}_n^{2+}$]$_2$, n = 2–6, in MeCN with 365 nm light.

complex narrows and its intensity increases (Fig. S1, Supplementary data), indicating that the stacking interactions become weaker because of increasing average distance between the stilbene moieties.

According to spectrophotometric titration data (Figs. S2 and S3, Supplementary data), the *Z* isomer of stilbene **1** forms highly stable 1:1 complexes with $\mathbf{C}_n^{2+}$, n = 2–6, in MeCN ($K_{1:1} > 10^7\ M^{-1}$). Fig. 2 (dashed curves) shows the absorption spectra of (*Z*)-**1** and complexes (*Z*)-**1**·$\mathbf{C_2}^{2+}$ and (*Z*)-**1**·($EtNH_3^+$)$_2$. The lowest-energy absorption band of (*Z*)-**1**·$\mathbf{C_2}^{2+}$ is strongly shifted toward shorter wavelengths relative to the corresponding bands of (*Z*)-**1** and (*Z*)-**1**·($EtNH_3^+$)$_2$. The only rational explanation for this finding is to assume a pseudocyclic structure of the 1:1 complex of (*Z*)-**1** with $\mathbf{C_2}^{2+}$. A similar assumption was made by Shinkai et al., on the basis of indirect observation, for complexes of (*Z*)-bis(18-crown-6) azobenzene with $\mathbf{C_2}^{2+}$ and $\mathbf{C_4}^{2+}$ (TsO^- as the counterion) in *n*-butanol–*o*-dichlorobenzene mixtures [20]. It was also demonstrated that (*Z*)-bis(crown)azobenzenes are able to form pseudocyclic 1:1 complexes with metal cations that are larger in diameter than the crown cavity; in these complexes, the metal cation is bound to both crown-ether moieties of azobenzene [21–23]. For example, the azobenzene analogue of (*Z*)-**1** forms a pseudocyclic 1:1 complex with the Cs^+ ion, the effective diameter of which (3.34 Å [24]) is smaller than the distance between the nitrogen atoms in $\mathbf{C_2}^{2+}$ (3.76 Å, as calculated by the M06-2X/6-31G(d)/SMD method).

The absorption spectra presented in Fig. S4 (Supplementary data) indicate that binding of $\mathbf{C}_n^{2+}$, n = 3–6, to (*Z*)-**1** also leads to the formation of pseudocyclic 1:1 complexes. The results of DFT calculations presented in Section 3.3 show that the peculiar spectral properties of the (*Z*)-**1**·$\mathbf{C}_n^{2+}$ complexes are mainly caused by large torsion angles around the ethylene–benzocrown single bonds.

It should be noted that the *E* isomer of stilbene **1** is also able to form highly stable pseudocyclic 1:1 complexes ($K_{1:1} > 10^7\ M^{-1}$) but with longer alkanediammonium ions, starting from 1,10-decanediammonium ion [25].

3.2. Photochemical properties

Stationary irradiation of complexes [(*E*)-**1**·$\mathbf{C}_n^{2+}$]$_2$, n = 2–6, in MeCN with 365 nm light resulted in complete consumption of (*E*)-**1** to give a mixture of photoproducts that show no absorption at λ = 365 nm, namely, complex (*Z*)-**1**·$\mathbf{C}_n^{2+}$ and cyclobutane **2** as complex **2**·($\mathbf{C}_n^{2+}$)$_2$. The photochemical and thermal processes occurring during the irradiation of complexes [(*E*)-**1**·$\mathbf{C}_n^{2+}$]$_2$ are shown in Scheme 3.

The absolute quantum yields of the PCA and *E*–*Z* photoisomerization reactions in complexes [(*E*)-**1**·$\mathbf{C}_n^{2+}$]$_2$ (φ_{PCA} and φ_{E-Z}, respectively) were determined in two stages. First, the total

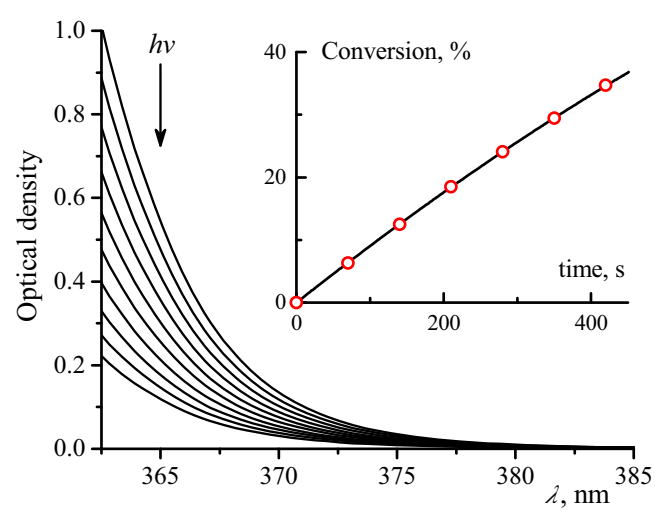

Fig. 3. Spectrophotometric data on the stationary photolysis of complex [(*E*)-**1**·$\mathbf{C_2}^{2+}$]$_2$ in MeCN with 365 nm light: (*E*)-**1** 3.4×10^{-4} M, $\mathbf{C_2}^{2+}2ClO_4^-$ 5.4×10^{-4} M, ionic strength 0.01 M ($Bu_4N^+ClO_4^-$), 1 cm cell, light intensity 1.3×10^{-9} mol cm^{-2} s^{-1}, irradiation time varied from 0 to 20 min. Inset: percentage of conversion of (*E*)-**1** as a function of the irradiation time; the solid curve is from global fitting to a kinetic equation for irreversible unimolecular photoreactions.

quantum yield for the conversion of (*E*)-**1** (φ_{tot}) was derived from the spectral kinetics observed at the long-wavelength edge of the absorption band of [(*E*)-**1**·$\mathbf{C}_n^{2+}$]$_2$ (Fig. 3, see also Figs. S5–S8, Supplementary data) where the photoproducts, *i.e.*, (*Z*)-**1**·$\mathbf{C}_n^{2+}$ and **2**·($\mathbf{C}_n^{2+}$)$_2$ show no absorption. The formation of intermediate complex (*Z*)-**1**·$\mathbf{C}_n^{2+}$·(*E*)-**1**·$\mathbf{C}_n^{2+}$ (Scheme 3) can be neglected for the case of low-intensity irradiation, because this complex rapidly dissociates ($\tau < 10$ s) to give pseudocyclic complex (*Z*)-**1**·$\mathbf{C}_n^{2+}$. The φ_{tot} value was determined by global fitting of spectrokinetic data in terms of the kinetic equation for irreversible unimolecular photoreactions [8].

The second stage was to determine the concentration ratio of the two photoproducts for different percentages of conversion of (*E*)-**1**. An accurate calculation of this ratio from the absorption spectrum of the photolysate was impossible, as the spectra of (*Z*)-**1**·$\mathbf{C}_n^{2+}$ and **2**·($\mathbf{C}_n^{2+}$)$_2$ overlap almost completely. Therefore, the photolysate samples taken at different percentages of conversion of (*E*)-**1** (from 0 to 70–80%) were diluted with a solution containing $Ba(ClO_4)_2$ (1×10^{-3} M) and the absorption spectra of the resulting three-component mixtures comprising (*E*)-**1**·(Ba^{2+})$_2$, (*Z*)-**1**·(Ba^{2+})$_2$, and **2**·(Ba^{2+})$_4$ were measured (see, for example, Fig. S9, Supplementary data). In addition, a sample taken after complete conversion of (*E*)-**1** was used to record the absorption spectrum of a two-component mixture of (*Z*)-**1**·(Ba^{2+})$_2$ and **2**·(Ba^{2+})$_4$. Complex (*Z*)-**1**·(Ba^{2+})$_2$ absorbs at longer wavelengths than complex **2**·(Ba^{2+})$_4$ (Fig. 4); therefore, the spectrum of **2**·(Ba^{2+})$_4$ could be easily derived by subtracting the known spectrum of (*Z*)-**1**·(Ba^{2+})$_2$ from the two-component mixture spectrum.

The absorption spectra of three-component mixtures of (*E*)-**1**·(Ba^{2+})$_2$, (*Z*)-**1**·(Ba^{2+})$_2$, and **2**·(Ba^{2+})$_4$ recorded in the 240–380 nm range were represented as the data matrix $\mathbf{D}_{exp}$ of the dimension $n \times m$, where m is the number of spectra and n is the number of optical density (D) values in the spectrum. This matrix was subjected to singular value decomposition (SVD). For each of the (*E*)-**1**–$\mathbf{C}_n^{2+}$ systems, the matrix $\mathbf{D}_{exp}$ was very well reconstructed using two principal SVD vectors; the standard deviation between the experimental and reconstructed matrices was less than 0.001 of optical density. This fact indicates that the mixture contains only two linearly independent light-absorbing components [26]. One of these components is complex (*E*)-**1**·(Ba^{2+})$_2$ and the other one is a mixture of complexes **2**·(Ba^{2+})$_4$ and (*Z*)-**1**·(Ba^{2+})$_2$ with a variable total concentration and invariable concentration ratio R_C = [**2**]/[(*Z*)-**1**]. The fact that R_C does not depend on the percentage of conversion of the *E* isomer during the photolysis of (*E*)-**1**–$\mathbf{C}_n^{2+}$ systems confirms the above mentioned assumption stating that (*E*)-**1** exists in these systems almost completely as bis-pseudosandwich complex [(*E*)-**1**·$\mathbf{C}_n^{2+}$]$_2$.

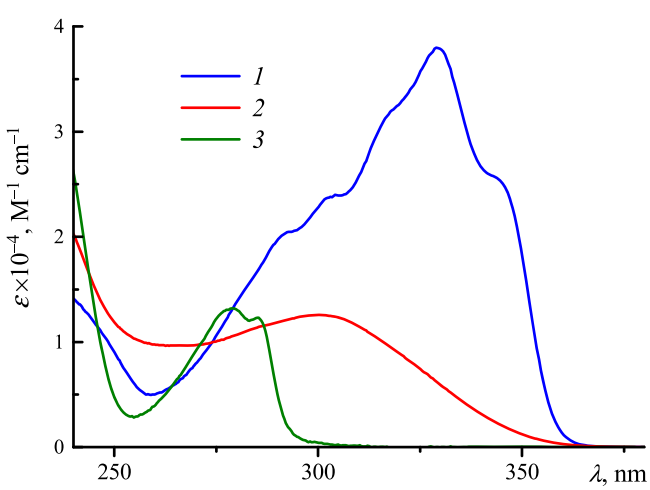

Fig. 4. Absorption spectra of complexes (*E*)-**1**·(Ba^{2+})$_2$ (*1*), (*Z*)-**1**·(Ba^{2+})$_2$ (*2*), and **2**·(Ba^{2+})$_4$ (*3*) in MeCN.

The R_C value was determined by parameterized modeling [26] of the matrix $\mathbf{D}_{exp}$ using the relation

$$D(\lambda) = \varepsilon_E(\lambda)[E]l + \{\varepsilon_Z(\lambda) + R_C\varepsilon_{cb}(\lambda)\}[Z]l$$

where $\varepsilon_E(\lambda)$, $\varepsilon_Z(\lambda)$, and $\varepsilon_{cb}(\lambda)$ are the known molar absorptivities of complexes (*E*)-**1**·(Ba^{2+})$_2$, (*Z*)-**1**·(Ba^{2+})$_2$, and **2**·(Ba^{2+})$_4$, respectively; [*E*] and [*Z*] are the concentrations of (*E*)-**1**·(Ba^{2+})$_2$ and (*Z*)-**1**·(Ba^{2+})$_2$; l is the cell length. The R_C value was found to increase with a decrease in the number of methylene units in $\mathbf{C}_n^{2+}$, namely, from 0.09 ($\mathbf{C_6}^{2+}$) to 2.3 ($\mathbf{C_2}^{2+}$).

When the values of R_C and φ_{tot} are known, it is easy to compute the quantum yields φ_{PCA} and φ_{E-Z}. The values of φ_{PCA} and φ_{E-Z} for complexes [(*E*)-**1**·$\mathbf{C}_n^{2+}$]$_2$ are summarized in Table 1.

As the length of the polymethylene spacers in the bis-pseudosandwich complex decreases, the efficiency of PCA reaction increases, while the quantum yield of *E–Z* photoisomerization decreases. The increase in φ_{PCA} is attributable to a decrease in the average distance between the two olefinic bonds in the complex and, perhaps, to a decrease in the number of complex conformations unfavorable for PCA. The decrease in φ_{E-Z} may be due to both the acceleration of the competing PCA reaction and increasing steric hindrance for *E–Z* photoisomerization in the pseudocyclic 2:2 complex. A certain role of steric factors in the *E–Z* photoisomerization of complexes [(*E*)-**1**·$\mathbf{C}_n^{2+}$]$_2$ is indicated by the fact that the φ_{E-Z} values for (*E*)-**1** and complex (*E*)-**1**·($EtNH_3^+$)$_2$, in which there is no steric hindrance for photoisomerization, are twice higher than that for complex [(*E*)-**1**·$\mathbf{C_6}^{2+}$]$_2$. It should be also noted that the PCA quantum yield of free (*E*)-**1** is negligibly small in comparison with the bis-pseudosandwich complexes, under the same experimental conditions.

3.3. DFT and TDDFT calculations

In order to confirm the conclusion that (*Z*)-**1** is able to form pseudocyclic 1:1 complexes even with short alkanediammonium ions such as $\mathbf{C_2}^{2+}$, we carried out DFT and TDDFT studies of (*Z*)-**1** and complexes (*Z*)-**1**·($EtNH_3^+$)$_2$ and (*Z*)-**1**·$\mathbf{C_2}^{2+}$ in MeCN. The structures of the most probable conformers of these compounds, as optimized by the M06-2X/6-31G(d)/SMD method, are presented in Fig. 5. The free energies in solution (G_{soln}), the binding free energies (ΔG_{bind}), and some other calculated energy quantities are collected in Table S1 (Supplementary data). The experimental and TDDFT calculated parameters of the S_0–S_1 electronic transition of these compounds are summarized in Table 2 (the calculated transition energies were corrected by a factor of 0.978).

In the C_2-symmetrical (*s-cis*)$_2$-(*dn*)$_2$ conformation of (*Z*)-**1** (Fig. 5A, conformational notation is given in Fig. 1), the torsion angles around the ethylene–benzocrown bond are 34.0°, and the bond lengths in the Ar—HC=CH moiety are 1.476 and 1.345 Å. The

Table 1
Quantum yields of the PCA and *E–Z* photoisomerization reactions in complexes [(*E*)-**1**·$\mathbf{C}_n^{2+}$]$_2$.[a]

Compound	φ_{tot}	φ_{PCA}	φ_{E-Z}
(*E*)-**1**			0.24[b]
[(*E*)-**1**·$\mathbf{C_2}^{2+}$]$_2$	0.33	0.27	0.06
[(*E*)-**1**·$\mathbf{C_3}^{2+}$]$_2$	0.28	0.21	0.07
[(*E*)-**1**·$\mathbf{C_4}^{2+}$]$_2$	0.23	0.13	0.10
[(*E*)-**1**·$\mathbf{C_5}^{2+}$]$_2$	0.12	0.02	0.10
[(*E*)-**1**·$\mathbf{C_6}^{2+}$]$_2$	0.14	0.02	0.12
(*E*)-**1**·($EtNH_3^+$)$_2$			0.26

[a] MeCN solution, irradiation with 365 nm light, the quantum yields are measured to within about ±20%.
[b] Ref. [27].

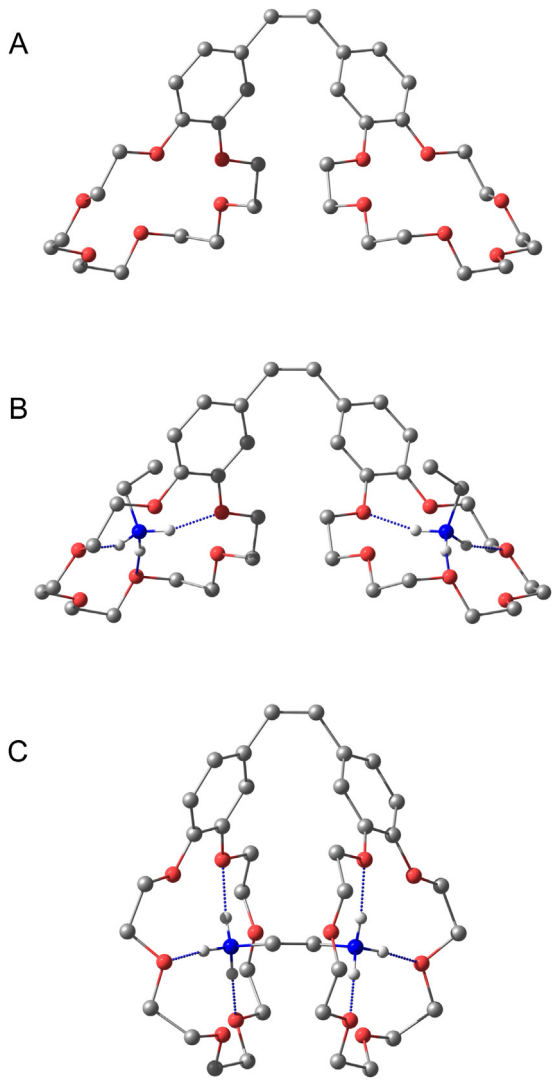

Fig. 5. Most probable conformations of (A) stilbene (*Z*)-**1**, (B) complex (*Z*)-**1**·$(EtNH_3^+)_2$, and (C) complex (*Z*)-**1**·$\mathbf{C_2}^{2+}$ in MeCN, as calculated by the M06-2X/6-31G (d)/SMD method; hydrogen atoms are not shown, except those of the ammonium groups.

Table 2
Experimental and TDDFT calculated parameters of the S_0–S_1 electronic transition of stilbene (*Z*)-**1** and its complexes with cations.[a]

Compound	λ_{max}	$\Delta\lambda_{max}$	ε_{max}	λ_{calc}[b]	$\Delta\lambda_{calc}$	f_{calc}
(*Z*)-**1**	304		12600	304		0.70
(*Z*)-**1**·$(EtNH_3^+)_2$	301	3	12400	300.5	3.5	0.69
(*Z*)-**1**·$(Ba^{2+})_2$	300	4	12500			
(*Z*)-**1**·$\mathbf{C_2}^{2+}$	280	24	12200	274.5	29.5	0.44

[a] In MeCN, λ_{max} (nm) is the position of the absorption maximum, ε_{max} ($M^{-1}cm^{-1}$) is the molar absorptivity at λ_{max}, $\Delta\lambda_{max} = \lambda_{max}$(ligand) − λ_{max}(complex), λ_{calc} (nm) is the calculated wavelength of the S_0–S_1 transition, f_{calc} is the oscillator strength, $\Delta\lambda_{cal} = \lambda_{cal}$(ligand) − λ_{cal}(complex).
[b] The calculated S_0–S_1 transition energies were corrected by a factor of 0.978.

corresponding (*s-cis*)$_2$-(*up*)$_2$ conformation of (*Z*)-**1** (Fig. S10A, Supplementary data) is less stable by only 0.3 kcal mol^{-1} and the λ_{calc} value for this conformation is larger by only 3 nm.

In the C_2-symmetrical (*s-cis*)$_2$-(*dn*)$_2$ conformation of (*Z*)-**1**·$(EtNH_3^+)_2$ (Fig. 5B), the main structural parameters of (*Z*)-**1** are very close to those of free (*Z*)-**1**; the torsion angles around the ethylene–benzocrown bonds are 34.3° and the bond lengths in the Ar—HC=CH moiety are 1.476 and 1.344 Å. The corresponding (*s-cis*)$_2$-(*up*)$_2$ conformation of (*Z*)-**1**·$(EtNH_3^+)_2$ (Fig. S10B) is virtually isoenergetic: the difference in G_{soln} was calculated to be 0.06 kcal mol^{-1}. Although the two conformations differ in the pattern of hydrogen bonds, they are characterized by very close wavelengths of the S_0–S_1 transition (the λ_{calc} value for the (*up*)$_2$ conformer is smaller by only 3 nm).

The most stable conformer of (*Z*)-**1**·$\mathbf{C_2}^{2+}$ (Fig. 5C) possesses nearly C_2 symmetry. The torsion angles around the ethylene–benzocrown bonds are about 46.6°, much greater than those in (*Z*)-**1** and (*Z*)-**1**·$(EtNH_3^+)_2$. The ethylene bond is somewhat more localized: the bond lengths in the Ar—HC=CH moiety are 1.482 and 1.342 Å. The C—C=C bond angles are about 124.4°, substantially smaller than those in (*Z*)-**1** (129.7°) and (*Z*)-**1**·$(EtNH_3^+)_2$ (129.7°). This is indicative of significant steric strain in pseudocyclic complex (*Z*)-**1**·$\mathbf{C_2}^{2+}$. The conformations of (*Z*)-**1**·$\mathbf{C_2}^{2+}$ with other patterns of hydrogen bonds, such as that shown in Fig. S10C, are much less stable (by more than 2 kcal mol^{-1}).

The TDDFT calculations predict well the experimental $\Delta\lambda_{max}$ values for both complexes. The exceptionally large value of $\Delta\lambda_{max}$ for (*Z*)-**1**·$\mathbf{C_2}^{2+}$ (24 nm) in comparison with (*Z*)-**1**·$(EtNH_3^+)_2$ (3 nm) and (*Z*)-**1**·$(Ba^{2+})_2$ (4 nm) is due to relatively large torsion angles around the ethylene–benzocrown bonds in the sterically strained pseudocyclic complex.

Another evidence for the pseudocyclic structure of (*Z*)-**1**·$\mathbf{C_2}^{2+}$ is the fact that the calculated binding free energy for this complex ($\Delta G_{bind} = -28.3$ kcal mol^{-1}) is higher than that for (*Z*)-**1**·$(EtNH_3^+)_2$ ($\Delta G_{bind} = -16.6$ kcal mol^{-1}). In both cases, the absolute binding energies are most likely overestimated due to underestimation of the solvation energies of the $EtNH_3^+$ and $\mathbf{C_2}^{2+}$ ions and due to basis set superposition errors.

3.4. Crystal structure of complex (E)-**1**·$\mathbf{C_6}^{2+}$·2ClO_4^-·2C_6H_6·MeCN

Fig. 6A shows the independent components of crystalline complex (*E*)-**1**·$\mathbf{C_6}^{2+}$·2ClO_4^-·2C_6H_6·MeCN (CCDC number 1510931, crystal data and details of the structure determination are presented in the Supplementary data). The disordered positions of some structural units, including the conformationally mobile crown-ether moieties of molecule (*E*)-**1**, decrease the reflectivity of the crystal and, hence, the accuracy of X-ray experiment. Nevertheless, the experimental accuracy was quite satisfactory, which allows us to discuss the subtle details of the structures of the components and the whole complex.

The ethylene bond in molecule (*E*)-**1** is largely localized: the bond lengths in the C(2)—C(1)=C(1A) unit are 1.471(4) and 1.320 (5) Å, respectively. The 18-membered macroheterocyclic moieties of (*E*)-**1** are in the typical crown-like conformation, most favorable for binding the primary ammonium ions. The N(1)H_3^+ group of the diammonium ion (as well as its symmetrical equivalent N(1A)H_3^+) is coordinated to the 18-crown-6 ether moiety of stilbene *via* the formation of three directional hydrogen bonds, N(1)H . . . O(1,3,5); the lengths of these bonds are 2.01, 1.92, and 2.04 Å, and the angles at hydrogen atoms are 176°, 175°, and 163°, respectively. These parameters correspond to a medium-strength hydrogen bond. The hexamethylene chain of the diammonium ion has a transoid conformation in which all carbon atoms are virtually in one plane parallel to the mean plane of the stilbene moiety of molecule (*E*)-**1**. However, the terminal groups CH_2CH_2—$CH_2NH_3^+$ have a *gauche* conformation, which is likely to be most favorable for efficient interaction of the ammonium group with the macrocycle.

In the (*E*)**1**·$\mathbf{C_6}^{2+}$·2ClO_4^-·2C_6H_6·MeCN structure, the stilbene molecule is arranged in a special position, so that the midpoint of the C(1)=C(1A) ethylene bond coincides with the center of symmetry of the crystal. The hexanediammonium ion also occupies a special position, and its midpoint coincides with another center of symmetry of the crystal. Therefore, the whole

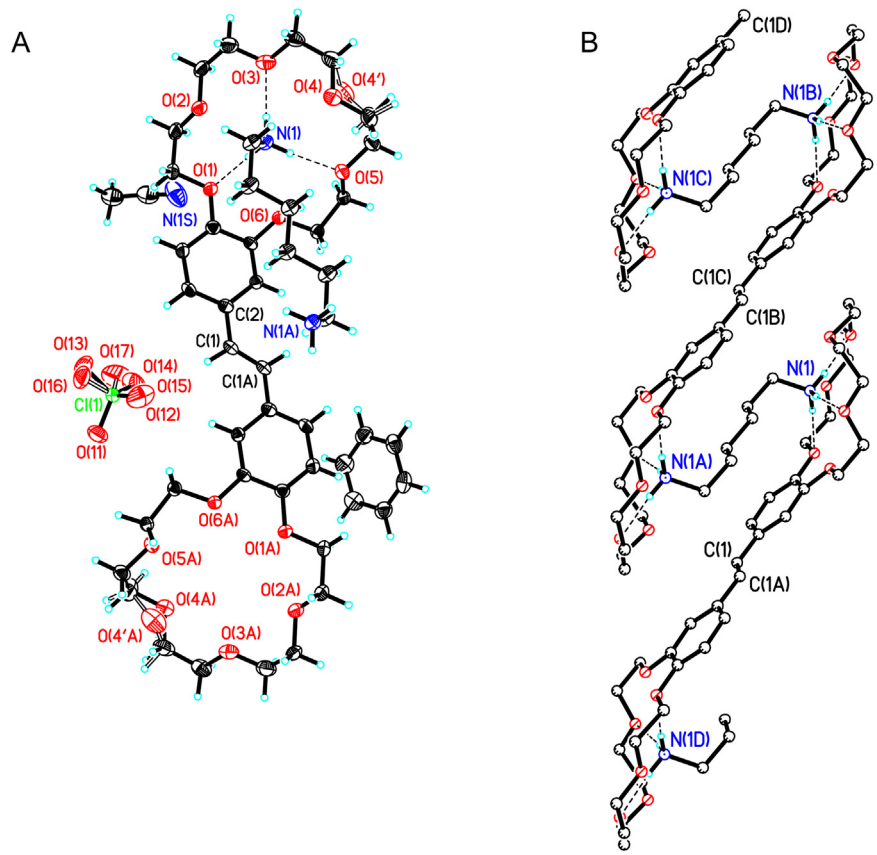

Fig. 6. A: Independent components of crystalline complex (*E*)-**1**·$\mathbf{C_6}^{2+}$·$2ClO_4^-$·$2C_6H_6$·MeCN; thermal ellipsoids are drawn at the 40% probability level; hydrogen bonds are shown by dash lines; additional letters "A" indicate that atoms belong to symmetrically related sites. B: Polymeric structure [(*E*)-**1**·$\mathbf{C_6}^{2+}$]$_n$ resulting from hydrogen bonding in the crystal; disordered fragments, perchlorate anions, solvate molecules, and most of the hydrogen atoms are omitted for clarity.

structure has a centrosymmetric type of connectivity, resulting, in particular, in an ideally planar conformation of the stilbene moiety in (*E*)-**1**. One more consequence of the centrosymmetric structure of the complex is that the ammonium groups are coordinated to the crown-ether moieties on different sides relative to the mean plane of stilbene moiety in (*E*)-**1**, and two NH_3^+ groups of one diammonium ion are linked to the crown-ether moieties of two (*E*)-**1** molecules. In the given space group ($P\overline{1}$), this inevitably leads to the formation of hydrogen-bonded polymeric structure, [(*E*)-**1**·$\mathbf{C_6}^{2+}$]$_n$ (Fig. 6B).

Thus, co-crystallization of stilbene (*E*)-**1** with 1,6-hexanediammonium diperchlorate does not lead to the formation of pseudocyclic 2:2 complexes, which are observed in dilute solutions. Instead, a linear supramolecular polymer [(*E*)-**1**·$\mathbf{C_6}^{2+}$]$_n$ with alternating (*E*)-**1** molecules and diammonium ions is formed. This indirectly indicates that in concentrated solutions, (*E*)-**1** and $\mathbf{C_6}^{2+}$ can form supramolecular assemblies of higher order than complexes [(*E*)-**1**·$\mathbf{C_6}^{2+}$]$_2$.

4. Conclusions

We elucidated the detailed picture of the hydrogen bond-directed self-assembly of bis(18-crown-6)stilbene and alkanediammonium ions of the structure $^+H_3N(CH_2)_nNH_3^+$, where $n = 2$–6, into supramolecular associates of different composition, such as pseudocyclic 2:2 complexes formed by the *E* isomer of bis(18-crown-6)stilbene. Also we determined how the number of methylene units in alkanediammonium ion affects the quantum yields of the [2 + 2] photocycloaddition and *E*–*Z* photoisomerization reactions occurring in the 2:2 complexes. The photocycloaddition quantum yield was found to increase with decreasing the number of methylene units, reaching the highest value (0.27) in the case of 1,2-ethanediammonium ion.

Generally, the efficiency of photocycloaddition in pseudocyclic structures in solution is dependent not only on the spacing and orientation of the reacting bonds but also on other factors, such as steric strain in the pseudocycle [8]. In the case of 2:2 complexes of (*E*)-bis(18-crown-6)stilbene, the spacing of the two olefinic bonds is likely to be the main factor affecting the photocycloaddition efficiency.

It was shown for the first time that the *Z* isomer of bis(18-crown-6)stilbene is able to form pseudocyclic 1:1 complexes even with very short alkanediammonium ions, such as 1,2-ethanediammonium ion. The peculiar spectral properties of these complexes arise from large torsion angles around the ethylene–benzocrown single bonds.

X-ray diffraction analysis revealed that co-crystallization of (*E*)-bis(18-crown-6)stilbene with 1,6-hexanediammonium diperchlorate affords a supramolecular polymer composed of alternating stilbene molecules and diammonium ions.

The results of this study can be used for the targeted design of photoactive supramolecular assemblies and for the development of photochemical synthesis of multitopic receptors such as tetracrown cyclobutanes.

Acknowledgements

This work was supported by the Russian Science Foundation (project no. 14-13-00076) and the Photochemistry Center, Russian Academy of Sciences (in respect of X-ray diffraction study of the

complex). L.G.K. thanks the Royal Society of Chemistry for International Author Grant.

Appendix A. Supplementary data

Supplementary data associated with this article can be found, in the online version, at http://dx.doi.org/10.1016/j.jphotochem.2017.03.003.

References

[1] N. Hoffmann, Photochemical reactions as key steps in organic synthesis, Chem. Rev. 108 (2008) 1052–1103, doi:http://dx.doi.org/10.1021/cr0680336.

[2] T. Bach, J.P. Hehn, Photochemical reactions as key steps in natural product synthesis, Angew. Chem. Int. Ed. 50 (2011) 1000–1045, doi:http://dx.doi.org/10.1002/anie.201002845.

[3] M.V. Alfimov, S.P. Gromov, O.B. Stanislavskii, E.N. Ushakov, O.A. Fedorova, Crown-containing styryl dyes. 8. Cation-dependent concerted [2 + 2] autophotocycloaddition of photochromic 15-crown-5 ether betaines, Russ. Chem. Bull. 42 (1993) 1385–1389, doi:http://dx.doi.org/10.1007/BF00699938.

[4] B. Bibal, C. Mongin, D.M. Bassani, Template effects and supramolecular control of photoreactions in solution, Chem. Soc. Rev. 43 (2014) 4179–4198, doi:http://dx.doi.org/10.1039/C3CS60366K.

[5] E.N. Ushakov, S.P. Gromov, Supramolecular methods for controlling intermolecular [2 + 2] photocycloaddition reactions of unsaturated compounds in solutions, Russ. Chem. Rev. 84 (2015) 787–802, doi:http://dx.doi.org/10.1070/RCR4514.

[6] E.N. Ushakov, A.I. Vedernikov, M.V. Alfimov, S.P. Gromov, Regio- and stereospecific [2 + 2] photocyclodimerization of a crown-containing butadienyl dye *via* cation-induced self-assembly in solution, Photochem. Photobiol. Sci. 10 (2011) 15–18, doi:http://dx.doi.org/10.1039/C0PP00227E.

[7] S.P. Gromov, A.I. Vedernikov, L.G. Kuz'mina, N.A. Lobova, S.S. Basok, Yu. A. Strelenko, M.V. Alfimov, Stereoselective [2 + 2] photocycloaddition in bispseudosandwich complexes of bis(18-crown-6) stilbene with alkanediammonium ions, Russ. Chem. Bull. 58 (2009) 108–114, doi:http://dx.doi.org/10.1007/s11172-009-0016-4.

[8] E.N. Ushakov, A.I. Vedernikov, N.A. Lobova, S.N. Dmitrieva, L.G. Kuz'mina, A.A. Moiseeva, J.A.K. Howard, M.V. Alfimov, S.P. Gromov, Supramolecular dimerization and [2+2] photocycloaddition reactions of crown ether styryl dyes containing a tethered ammonium group: structure-property relationships, J. Phys. Chem. A 119 (2015) 13025–13037, doi:http://dx.doi.org/10.1021/acs.jpca.5b10758.

[9] A.I. Vedernikov, E.N. Ushakov, N.A. Lobova, A.A. Kiselev, M.V. Alfimov, S.P. Gromov, Photosensitive molecular tweezers. 3. Synthesis and homoditopic complex formation of a bisstyryl dye containing two crown-ether fragments with diammonium salts, Russ. Chem. Bull. 54 (2005) 666–672, doi:http://dx.doi.org/10.1007/s11172-005-0303-7.

[10] A.I. Vedernikov, S.S. Basok, S.P. Gromov, L.G. Kuz'mina, V.G. Avakyan, N.A. Lobova, E. Yu. Kulygina, T.V. Titkov, Yu. A. Strelenko, E.I. Ivanov, J.A.K. Howard, M.V. Alfimov, Synthesis and structure of bis-crown-containing stilbenes, Russ. J. Org. Chem. 41 (2005) 843–854, doi:http://dx.doi.org/10.1007/s11178-005-0255-2.

[11] G. Lindsten, O. Wennerström, B. Thulin, Stilbene bis-crown ethers: synthesis, complexation and photoisomerization, Acta Chem. Scand. B40 (1986) 545–554, doi:http://dx.doi.org/10.3891/acta.chem.scand.40b-0545.

[12] D.N. Laikov, A new parametrizable model of molecular electronic structure, J. Chem. Phys. 135 (2011) 134120–134130, doi:http://dx.doi.org/10.1063/1.3646498.

[13] D.N. Laikov, Priroda, Quantum Chemical Program, Version 2014.02.23, Lomonosov Moscow State University, Moscow, 2014. http://rad.chem.msu.ru/~laikov/.

[14] M.J. Frisch, G.W. Trucks, H.B. Schlegel, G.E. Scuseria, M.A. Robb, J.R. Cheeseman, G. Scalmani, V. Barone, B. Mennucci, G.A. Petersson, H. Nakatsuji, M. Caricato, X. Li, H.P. Hratchian, A.F. Izmaylov, J. Bloino, G. Zheng, J.L. Sonnenberg, M. Hada, M. Ehara, K. Toyota, R. Fukuda, J. Hasegawa, M. Ishida, T. Nakajima, Y. Honda, O. Kitao, H. Nakai, T. Vreven, J.A. Montgomery Jr., J.E. Peralta, F. Ogliaro, M. Bearpark, J.J. Heyd, E. Brothers, K.N. Kudin, V.N. Staroverov, T. Keith, R. Kobayashi, J. Normand, K. Raghavachari, A. Rendell, J.C. Burant, S.S. Iyengar, J. Tomasi, M. Cossi, N. Rega, J.M. Millam, M. Klene, J.E. Knox, J.B. Cross, V. Bakken, C. Adamo, J. Jaramillo, R. Gomperts, R.E. Stratmann, O. Yazyev, A.J. Austin, R. Cammi, C. Pomelli, J.W. Ochterski, R.L. Martin, K. Morokuma, V.G. Zakrzewski, G.A. Voth, P. Salvador, J.J. Dannenberg, S. Dapprich, A.D. Daniels, O. Farkas, J.B. Foresman, J.V. Ortiz, J. Cioslowski, D.J. Fox, Gaussian 09, Revision D. 01, Gaussian, Inc, Wallingford, CT, 2013.

[15] Y. Zhao, D.G. Truhlar, The M06 suite of density functionals for main group thermochemistry, thermochemical kinetics, noncovalent interactions, excited states, and transition elements: two new functionals and systematic testing of four M06-class functionals and 12 other functionals, Theor. Chem. Acc. 120 (2008) 215–241, doi:http://dx.doi.org/10.1007/s00214-007-0310-x.

[16] A.V. Marenich, C.J. Cramer, D.G. Truhlar, Universal solvation model based on solute electron density and on a continuum model of the solvent defined by the bulk dielectric constant and atomic surface tensions, J. Phys. Chem. B 113 (2009) 6378–6396, doi:http://dx.doi.org/10.1021/jp810292n.

[17] J. Ho, A. Klamt, M.L. Coote, Comment on the correct use of continuum solvent models, J. Phys. Chem. A 114 (2010) 13442, doi:http://dx.doi.org/10.1021/jp107136j.

[18] G. Scalmani, M.J. Frisch, B. Mennucci, J. Tomasi, R. Cammi, V. Barone, Geometries and properties of excited states in the gas phase and in solution: theory and application of a time-dependent density functional theory polarizable continuum model, J. Chem. Phys. 124 (2006) 094107, doi:http://dx.doi.org/10.1063/1.2173258.

[19] S.P. Gromov, A.I. Vedernikov, N.A. Lobova, L.G. Kuz'mina, S.S. Basok, Yu. A. Strelenko, M.V. Alfimov, J.A.K. Howard, Controlled self-assembly of bis(crown) stilbenes into unusual bis-sandwich complexes: structure and stereoselective [2 + 2] photocycloaddition, New J. Chem. 35 (2011) 724–737, doi:http://dx.doi.org/10.1039/C0NJ00780C.

[20] S. Shinkai, T. Yoshida, O. Manabe, Y. Fuchita, Photoresponsive crown ethers. Part 20. Reversible photocontrol of association–dissociation equilibria between azobis(benzo-18-crown-6) and diammonium cations, J. Chem. Soc., Perkin Trans. 1 (1988) 1431–1437, doi:http://dx.doi.org/10.1039/P19880001431.

[21] S. Shinkai, T. Ogawa, Y. Kusano, O. Manabe, Selective extraction of alkali metal cations by a photoresponsive bis(crown ether), Chem. Lett. 9 (1980) 283–286, doi:http://dx.doi.org/10.1246/cl.1980.283.

[22] S. Shinkai, T. Nakaji, T. Ogawa, K. Shigematsu, O. Manabe, Photoresponsive crown ethers. 2. Photocontrol of ion extraction and ion transport by a bis (crown ether) with a butterfly-like motion, J. Am. Chem. Soc. 103 (1981) 111–115, doi:http://dx.doi.org/10.1021/ja00391a021.

[23] S. Shinkai, T. Ogawa, Y. Kusano, O. Manabe, K. Kikukawa, T. Goto, T. Matsuda, Photoresponsive crown ethers. 4. Influence of alkali metal cations on photoisomerization and thermal isomerization of azobis(benzocrown ethers), J. Am. Chem. Soc. 104 (1982) 1960–1967, doi:http://dx.doi.org/10.1021/ja00371a027.

[24] R.D. Shannon, Revised effective ionic radii and systematic studies of interatomic distances in halides and chalcogenides, Acta Crystallogr. A32 (1976) 751–767, doi:http://dx.doi.org/10.1107/S0567739476001551.

[25] E.N. Ushakov, S.P. Gromov, A.I. Vedernikov, E.V. Malysheva, A.A. Botsmanova, M.V. Alfimov, B. Eliasson, U.G. Edlund, J.K. Whitesell, M.A. Fox, Self-organization of highly stable electron donor-acceptor complexes via host-guest interactions, J. Phys. Chem. A 106 (2002) 2020–2023, doi:http://dx.doi.org/10.1021/jp012082z.

[26] E.N. Ushakov, S.P. Gromov, O.A. Fedorova, Yu. V. Pershina, M.V. Alfimov, F. Barigelletti, L. Flamigni, V. Balzani, Sandwich-type complexes of alkaline-earth metal cations with a bisstyryl dye containing two crown ether units, J. Phys. Chem. A 103 (1999) 11188–11193, doi:http://dx.doi.org/10.1021/jp9929420.

[27] E.N. Ushakov, V.A. Nadtochenko, S.P. Gromov, A.I. Vedernikov, N.A. Lobova, M. V. Alfimov, F.E. Gostev, A.N. Petrukhin, O.M. Sarkisov, Ultrafast excited state dynamics of the bi- and termolecular stilbene-viologen charge-transfer complexes assembled via host-guest interactions, Chem. Phys. 298 (2004) 251–261, doi:http://dx.doi.org/10.1016/j.chemphys.2003.12.002.